Synthesis and structural characterization of $ASnFe(PO_4)_3$ ($A=Na_2$,Ca,Cd) phosphates with the Nasicon type structure

Abderrahim Aatiq[a)]
Département de Chimie, Laboratoire de Chimie des Matériaux Solides, Faculté des Sciences Ben M'Sik, Avenue Idriss El harti, B.P. 7955, Casablanca, Morocco

(Received 10 November 2003; accepted 8 March 2004)

The crystal structures of $ASnFe(PO_4)_3$ ($A=Na_2$, Ca, Cd) phases, obtained by conventional solid state reaction techniques at (950–1000 °C), were determined at room temperature from X-ray powder diffraction (XRD) using Rietveld analysis. The three materials exhibit the Nasicon-type structure ($R\bar{3}c$ space group, $Z=6$) with a random distribution of Sn(Fe) within the framework. Hexagonal cell parameters when $A=Na_2$, Ca and Cd are: $a=8.628(1)$ Å, $c=22.151(2)$ Å; $a=8.569(1)$ Å, $c=22.037(2)$ Å and $a=8.587(1)$ Å, $c=21.653(2)$ Å, respectively. Structural refinements show a partial occupancy of M1 (Na(1)) and M2 (Na(2)) sites in $Na_2SnFe(PO_4)_3$ leading to the cationic distribution $[Na_{1.22}\square_{1.78}]_{M2}[Na_{0.78}\square_{0.22}]_{M1}SnFe(PO_4)_3$. Ca^{2+} ions are distributed only in the M1 site of $[\square_3]_{M2}[Ca]_{M1}SnFe(PO_4)_3$. From XRD data, it is difficult to unambiguously distinguish between Cd^{2+} and Sn^{4+} ions in $CdSnFe(PO_4)_3$. Nevertheless the overall set of cation–anion distances within the Nasicon framework clearly shows that the cationic distribution can be illustrated by the $[\square_3]_{M2}[Cd]_{M1}SnFe(PO_4)_3$ crystallographic formula. Distortion within the $[Sn(Fe)(PO_4)_3]$ frameworks, in $ASnFe(PO_4)_3$ ($A=Na_2$,Ca,Cd) phases, is shown to be related to the M1 site size.
[DOI: 10.1154/1.1725232]

I. INTRODUCTION

Materials with the general formula $A_xBB'(PO_4)_3$ consisting of a $BB'(PO_4)_3$ framework built up by a corner-sharing $B(B')O_6$ octahedra and PO_4 tetrahedra in such a way that each octahedron is surrounded by six tetrahedra and each tetrahedron is connected to four octahedra, crystallise mainly in the Nasicon $NaZr_2(PO_4)_3$ ($R\bar{3}c$ space group) (Hagman and Kierkegaard, 1968) or the langebeinite $Na_2TiB'(PO_4)_3$ ($B'=Cr,Fe$) structures ($P2_13$ space group) (Isasi and Daidouh, 2000). Depending on the temperature of preparation, the Nasicon structure can transform to the langbeinite as it was shown for $BaTiV(PO_4)_3$ (Kasthuri Rangan and Gopalakrishnan, 1994). Both structure types are related to each other by simple distortions and/or rotations of the cations polyhedra. The langbeinite structure is a cage structure with large A cations in the cages and small windows connecting the cages. Within the Nasicon framework, there are interconnected interstitial sites usually labeled M1 and M2 through which A cation can diffuse, giving rise to a fast-ion conductivity (Hong, 1976; Delmas *et al.*, 1981; Aatiq *et al.*, 2002a).

Phosphates within the Nasicon-type family have been the subject of intensive research due to their potential applications as a solid electrolyte, electrode material, and low thermal expansion ceramics (Hong, 1976; Padhi *et al.*, 1997; Delmas *et al.*, 1988; Woodcock *et al.*, 1999; Aatiq *et al.*, 2002b). Previously, there was particular interest by several authors in the phosphates with Nasicon-type materials especially those containing, within the framework, elements which can have more than one oxidation state (e.g., Ti, Fe, Sn, Nb, V) (Morin *et al.*, 1997; Masquelier *et al.*, 2000; Aatiq *et al.*, 2002a; Yin *et al.*, 2003). More recently, the structural characteristics by powder X-ray diffraction (XRD) study using the Rietveld method for the two $ATiFe(PO_4)_3$ ($A=Ca,Cd$) phases were realised (Aatiq and Dhoum, 2003). In both materials, A^{2+} cations are distributed in the M1 site and $Fe^{3+}(Ti^{4+})$ within the Nasicon $Ti(Fe)(PO_4)_3$ framework. In a continuation of our search concerning Nasicon-like structure, the first objective of the present study was the structural determination, using Rietveld refinement of the XRD patterns, of $CaSnFe(PO_4)_3$. Our work has therefore been extended to the structural study of two newly synthesised phases with general formula $ASnFe(PO_4)_3$ ($A=Na_2$,Cd).

II. EXPERIMENTAL

Syntheses of $ASnFe(PO_4)_3$ ($A=Na_2$,Ca,Cd) were carried out using conventional solid-state reaction techniques. Powder crystalline samples were prepared from mixtures of carbonates Na_2CO_3 (Merck, 99.5%) or $CaCO_3$ (Riedel-de Haën, 99%) or $CdCO_3$ (Riedel-de Haën, 99%), oxides SnO_2 (Riedel-de Haën, 99.9%), Fe_2O_3 (Prolabo, 99%), and $NH_4H_2PO_4$ (Riedel-de Haën, 99%) in stoichiometric proportions. The mixture was heated progressively with intermittent grinding at 200 °C (12 h), 600 °C (12 h), 800 °C (16 h), 950 °C (48 h) for ($A=Na_2$) and another treatment at 1000 °C (48 h) for ($A=Ca,Cd$) in air atmosphere. The products of reaction were characterised by XRD at room temperature with a Bruker D8 advance (θ–2θ) diffractometer; ($Cu\,K\alpha$) radiation (40 kV, 40 mA); divergence slit of 1° and antiscatter slit of 1°. The data were collected in the 10°–90° (2θ) range by steps of 0.02°(2θ), with a constant counting time of 14 s by step. The refinement of the structure by the Rietveld method was performed using the FULLPROF program (Rodriguez-Carvajal, 1997).

a) Electronic mail: a_aatiq@yahoo.fr

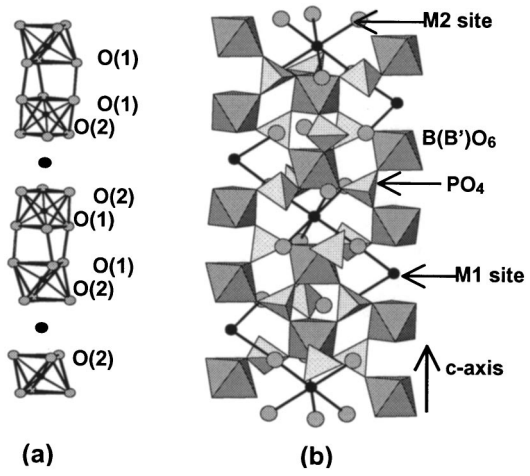

Figure 1. Crystal structure of the rhombohedral ($R\bar{3}c$ space group) $[M2]_3[M1]BB'(PO_4)_3$ Nasicon-type: perspective view of a part of the Nasicon ribbon in (a); M1 and M2 site are visualized in (b).

III. RESULTS AND DISCUSSION

XRD powder data of the three $ASnFe(PO_4)_3$ ($A = Na_2, Ca, Cd$) phases indicated that they were highly crystalline with their structure belonging to the rhombohedral $R\bar{3}c$ Nasicon type. Therefore, the following structural refinements were based upon this assumption.

It should be noticed that within the Nasicon framework, there are four interconnected cation sites, per formula unit, usually labeled M1 (one per formula unit) and M2 (three per formula unit) which can be represented by the crystallographic $[M2]_3[M1]BB'(PO_4)_3$ formula. Within the $[BB'(PO_4)_3]$ skeleton, each M1 cavity is situated between two $B(B')O_6$ octahedra along the *c* axis at the intersection of three conduction channels (Figure 1). Six M2 cavities with eightfold coordination are located between the $[O_3B(B')O_3M1O_3B(B')O_3\ O_3B(B')O_3]_\infty$ ribbons and surround the M1 cavity.

A. Rietveld refinement

Initial starting parameters for the Rietveld refinement of $Na_2SnFe(PO_4)_3$ were based on those already reported for the $R\bar{3}c$ structure of $[Li_{0.5}\square_{2.50}]_{M2}[Li_{0.50}Mn_{0.50}]_{M1}TiCr(PO_4)_3$ (Aatiq *et al.*, 1998). In the first step, we have assumed that Sn and Fe atoms were randomly distributed within the Nasicon framework [i.e., Sn(Fe) in the Ti(Cr) site]. The structural parameters of $CaTiFe(PO_4)_3$ (Aatiq and Dhoum, 2003) were used as starting parameters for the Rietveld refinement of the two $ASnFe(PO_4)_3$ ($A = Ca, Cd$) phases. Even if the divalent ions in $A^{2+}B^{4+}B'^{3+}(PO_4)_3$ type phases occupied preferentially the M1 sites of the Nasicon framework (Aatiq *et al.*, 1998; Aatiq and Dhoum, 2003) in a first step of the structural refinement, A ($A = Ca, Cd$), Fe, and Sn atoms were separately supposed to be distributed in the M1 sites. As will be discussed in the following, hypothesis of possible occupation of the M2 sites in $ASnFe(PO_4)_3$ Nasicon framework was also checked.

B. Structure of $Na_2SnFe(PO_4)_3$

Structural refinement of $Na_2SnFe(PO_4)_3$ was made in two principle steps. In the first step, full occupancy of the M1 site (one Na atom per formula unit), at (000) 6b position, and the excess of sodium (one Na atom per formula unit) located in the M2 site, at (0.62 0 1/4) (18e), was postulated. In this case, refinement leads to a large value (8(1) Å^2) of the displacement parameter, B_{iso}, of sodium Na(1) in M1 sites and a value of ($-0.9(1)$ Å^2) for Na(2) in M2 sites. Therefore, in the second step of the refinement the occupancies of Na(1) and Na(2) sites were allowed to vary, but the total sodium contents were constrained to 2. The result of the Rietveld refinement, reported in Table I, shows clearly a partial occupancy of M1 sites thus leading to the crystallographic $[Na_{1.22}\square_{1.78}]_{M2}[Na_{0.78}\square_{0.22}]_{M1}SnFe(PO_4)_3$ formula. It should be noticed that the possible distribution of Na^+ within the Nasicon framework was already shown for example in $Na_5Ti(PO_4)_3$ Nasicon phase $[[Na_3]_{M2}[Na]_{M1}TiNa(PO_4)_3$ crystallographic formula]

TABLE I. Results of the Rietveld refinement of $Na_2SnFe(PO_4)_3$.

$Na_2SnFe(PO_4)_3 = ([Na_{1.22}\square_{1.78}]_{M2}[Na_{0.78}\square_{0.22}]_{M1}SnFe(PO_4)_3)$
Space group, *R3c;* [$Z = 6$, $a_{hex} = 8.628(1)$ Å; $c_{hex} = 22.151(2)$ Å; $V = 1428(1)$ Å^3]
Experimental data
Temperature, 298 K; angular range, $10° \leqslant 2\theta \leqslant 90°$; step scan increment ($2\theta$), 0.02°
Zero point (2θ), $-0.061(2)°$; number of fitted parameters, 30
Profile parameters
Pseudo-Voigt function, $PV = \eta L + (1-\eta)G$; $\eta = 0.949(2)$
Polynomial function for the background (six parameters)
Half-width parameters, $U = 0.087(2)$, $V = -0.013(5)$, and $W = 0.0049(5)$
Conventional Rietveld *R*-factors, $R_{WP} = 5.8\%$; $R_P = 4.3\%$; $R_B = 5.6\%$; $R_F = 5.0\%$

Atom	Site	Wyckoff positions			B_{iso} (Å^2)	Occupancy
Na(1)	6b	0	0	0	2.9(5)	0.78(2)
Na(2)	18e	0.6304(6)	0	0.25	4.3(6)	0.407(1)
Sn(Fe)	12c	0	0	0.1466(1)	0.34(6)	1
P	18e	0.2895(8)	0	0.25	1.9(2)	1
O(1)	36f	0.177(5)	0.9751(6)	0.1941(5)	2.1(2)	1
O(2)	36f	0.1896(8)	0.1598(6)	0.0850(5)	2.1(2)	1

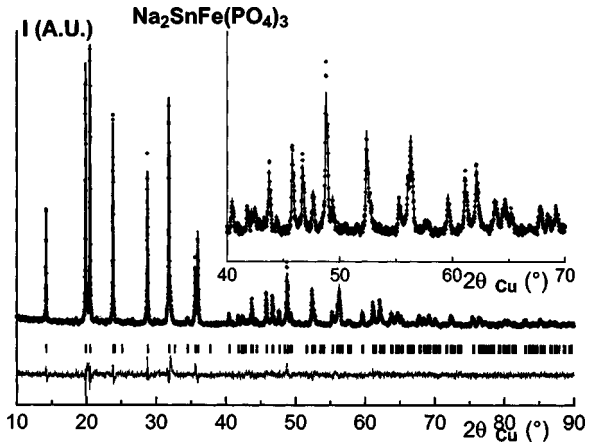

Figure 2. Experimental (···) calculated (—), and difference profile of the XRD pattern of $Na_2SnFe(PO_4)_3$.

(Krimi *et al.*, 1993). Therefore, the structural refinement of $Na_2SnFe(PO_4)_3$ was reconsidered in order to check whether or not the sodium atoms are localised within the Nasicon framework. For that reason, two main hypotheses of refinements were verified: (i) all Fe atoms in the M1 sites and Sn(Na) within the Nasicon framework and (ii) all Sn atoms in M1 sites and Fe(Na) within the Nasicon framework. In both cases larger values of the Bragg reliability factors and displacement parameters ($[Na_1\square_2]_{M2}[Fe]_{M1}SnNa(PO_4)_3$; e.g., $R_B=9.2\%$ and $B(Fe)_{M1}=77$ (Å^2)) and ($[Na_1\square_2]_{M2}[Sn]_{M1}NaFe(PO_4)_3$; e.g., $B(Sn)_{M1}=95$ (Å^2) and $R_B=16.3\%$)) were obtained. Therefore, only the hypothesis of distribution of Sn(Fe) within the Nasicon framework was retained. A comparison of the experimental and calculated XRD profile of $Na_2SnFe(PO_4)_3$ is shown in Figure 2. Note that the overall set of distances within the framework [Sn(Fe)–O(1) = 1.953(4) Å, Sn(Fe)–O(2) = 2.045(4) Å, and Na(1)–O(2) = 2.422(2) Å] is in good agreement with the ionic radii values in six coordination ($r_{Sn^{4+}}=0.69$ Å, $r_{Fe^{3+}}=0.645$ Å, $r_{Na^{+}}=1.02$ Å) (Shannon, 1976). P–O distances 1.521(3) Å; 1.562(3) Å] are comparable to those generally found in Nasicon-like phosphate. In M2 sites, the sodium is bounded by eight oxygen with Na(2)–O distance values of [2.300(5); 2.444(4); 2.684(3); 2.858(3) Å]. In order to have more structural information, the bond valence sums (BVS) based on bond-strength analysis (Brown and Altermatt, 1985) for $Na_2SnFe(PO_4)_3$ were computed. The BVS values calculated for Na, Fe, Sn, and P sites [1.1

TABLE II. Powder diffraction data of $Na_2SnFe(PO_4)_3$ (Cu $K\alpha_1$; $\lambda = 1.540\,56$ Å).[a]

hkl	d_{obs} (Å)	$100I/I_0$ (obs)	$100I/I_0$ (calc)	*hkl*	d_{obs} (Å)	$100I/I_0$ (obs)	$100I/I_0$ (calc)
012	6.1943	32	32	146	1.4916	11	10
104	4.4492	89	90	0 3 12	1.4831	1	1
110	4.3141	100	100	238	1.4575	2	2
113	3.7249	77	77	2 0 14	1.4534	9	9
006	3.6916	1	1	3 1 11	1.4442	1	1
024	3.0972	63	62	054	1.4428	6	6
116	2.8050	83	81	330	1.4380	7	7
211	2.8015	7	6	4 0 10	1.4280	7	7
018	2.5964	2	2	1 1 15	1.3972	2	2
214	2.5159	29	26	1 2 14	1.3804	9	8
300	2.4907	21	23	244	1.3683	5	5
208	2.2246	4	5	3 2 10	1.3557	6	6
220	2.1570	3	4	336	1.3400	3	3
119	2.1378	3	4	511	1.3396	1	1
1 0 10	2.1238	4	4	514	1.3043	10	9
217	2.1071	1	1	0 2 16	1.2982	1	1
223	2.0705	4	3	428	1.2580	1	1
036	2.0648	8	8	3 1 14	1.2576	5	5
312	2.0371	1	3	600	1.2454	3	3
128	1.9772	18	18	2 1 16	1.2431	1	1
134	1.9409	17	15	517	1.2355	1	1
0 2 10	1.9054	9	9	0 0 18	1.2306	2	2
226	1.8624	36	34	342	1.2209	1	1
0 0 12	1.8460	2	2	434	1.1993	1	1
042	1.8420	4	5	250	1.1965	2	2
2 1 10	1.7430	25	26	2 4 10	1.1907	3	3
137	1.7337	5	5	2 3 14	1.1627	6	6
318	1.6592	8	9	5 1 10	1.1478	1	1
324	1.6376	14	14	256	1.1382	2	2
140	1.6306	12	12	526	1.1382	4	4
235	1.5987	1	1	348	1.1229	4	4
413	1.5922	2	2	1 5 11	1.1168	1	1
048	1.5486	3	3	164	1.1161	2	2
0 1 14	1.5479	6	7	3 0 18	1.1033	1	1
1 3 10	1.5134	17	16	0 1 2	1.0956	3	3

[a]Diffraction lines with $I_{obs}<1$ are omitted.

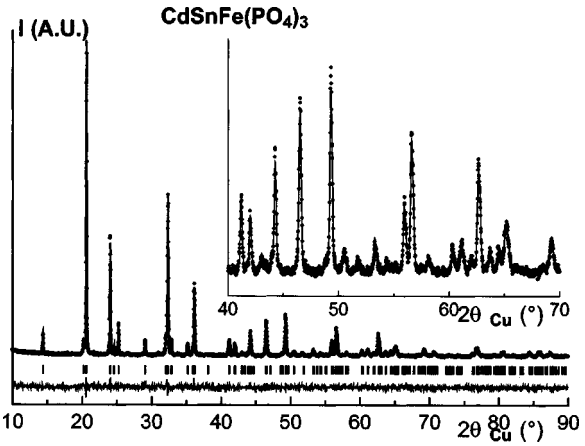

Figure 3. Experimental (···) calculated (—), and difference profile of the XRD pattern of $CdSnFe(PO_4)_3$.

for Na(1) in the M1 site, 1.1 for Na(2) in the M2 site, 3.8 (should be 3.5) for Sn/Fe, and 4.9 for P] are relatively consistent with the expected formal oxidation state of Na^+, Fe^{3+}, Sn^{4+}, and P^{5+} ions. X-ray powder diffraction data of $Na_2SnFe(PO_4)_3$, obtained from the "observed intensities" of the Rietveld refinement (Cu $K\alpha$1:1.540 56 Å), are presented in Table II.

C. Structure of $CdSnFe(PO_4)_3$

The fact that the amplitude of X-ray scattering by an element is proportional to its atomic number sets a severe limitation on the amount of information which can be obtained by X-ray investigations of substances containing atoms of neighbouring atomic number. On the basis of XRD data alone therefore it is not possible in our case to distinguish without ambiguity between Cd and Sn atoms. Since only the XRD data are available and Sn^{4+} and Cd^{2+} are isoelectronic ions, three hypotheses of Cd, Sn, and Fe atoms distribution, in $CdSnFe(PO_4)_3$, were checked. Refinement with all Fe atom in M1 site and Sn(Cd) within the Nasicon-framework, $[\square_3]_{M2}[Fe]_{M1}SnCd(PO_4)_3$, leads to very high reliability factors especially for R_B (R_B=22.3%) and also unacceptable displacement parameters [e.g., B_{iso}(Fe) $=-6.4$ Å^2; B_{iso}(Sn/Cd)$=8.5$ Å^2]. This first refinement indirectly indicates that Fe atoms are located within the framework. In the second hypothesis, refinement with all Sn in M1 sites and Fe(Cd) atoms within the framework, $[\square_3]_{M2}[Sn]_{M1}CdFe(PO_4)_3$, leads to a displacement parameters B_{iso}(Cd/Fe) of -0.14 Å^2 and acceptably reliability factors but a Sn–O(2) distance value (2.350 Å) which is very high in comparison to that expected from the ionic radii of Sn^{4+} and O^{2-} (2.09 Å). As it was expected, unacceptable BVS values were obtained from this hypothesis of cationic distributions ($[\square_3]_{M2}[Sn]_{M1}CdFe(PO_4)_3$, e.g., BVS=1.8 for Sn^{4+} ions). In the third hypothesis, refinement with all Cd atoms in M1 sites $[\square_3]_{M2}[Cd]_{M1}SnFe(PO_4)_3$, leads to relatively best results. Even if the consistency of $Cd_{M1}-O(2)$ interatomic distance value [2.338(2) Å], obtained at this stage of refinement, with that calculated from Shannon's Tables, the structural refinement of $CdSnFe(PO_4)_3$ was therefore reconsidered, with Cd atoms only in M1 site, but in this case the Cd^{2+} ions' content were allowed to vary. This last model leads to an occupancy rate value of 0.97(1) for Cd^{2+} ions in M1 sites and relatively little changes in the atomic positions. As will be shown in the following, even if this last model suspects the cadmium stoichiometry in this material, it leads to the best result. The same behaviour was already encountered in $CdTiFe(PO_4)_3$ Nasicon phase (Aatiq and Dhoum, 2003). Note that refinement considering the simultaneous occupation of both M1 and M2 sites by Cd^{2+} ions leads to a small and physically insignificant value of the occupancy factor (Occ) for M2(18e) (~0.63, 0, 0.25) sites ($Occ_{M2}=0.001$). Therefore, Cd^{2+} ions were considered to be exclusively distributed within the M1 sites of the Nasicon structure. The fitted XRD profile and the final atomic parameters are given in Figure 3 and Table III, respectively. Cd–O(2) distance value [2.305(2) Å] is consistent with the ionic radii of Cd^{2+} and O^{2-} ions ($r_{Cd^{2+}}=0.95$ Å, $r_{O^{2-}}=1.40$ Å). Sn(Fe)–O distances [1.962(3); 2.062(2) Å] show a 3+3 distortion of the $Sn(Fe)O_6$ octahedra. P–O distance values, 1.502(2) and 1.565(2) Å, are comparable to those generally found in Nasicon-like phosphate. The BVS values calculated for Cd,

TABLE III. Results of the Rietveld refinements of $CdFeSn(PO_4)_3$.

$[Cd]_{M1}SnFe(PO_4)_3$
Space group, $R\bar{3}c$; [$Z=6$; $a_{hex}=8.587(1)$ Å; $c_{hex}=21.653(2)$ Å; $V=1383(1)$ Å^3]
Experimental data
Temperature: 298 K; angular range, $10° \leqslant 2\theta \leqslant 90°$; step scan increment ($2\theta$), 0.02°
Zero point (2θ), $-0.063(2)$°; number of fitted parameters, 29
Profile parameters
Pseudo-Voigt function, $PV=\eta L+(1-\eta)G$; $\eta=0.544(3)$
Polynomial function for the background (six parameters)
Half-width parameters, $U=0.077(4)$, $V=0.037(5)$, and $W=0.0011(1)$
Conventional Rietveld R-factors, $R_{WP}=5.2\%$; $R_P=4.1\%$; $R_B=3.4\%$; $R_F=4.7\%$

Atom	Site	Wyckoff positions			B_{iso} (Å^2)	Occupancy
Cd	6b	0	0	0	1.9(1)	0.97(1)
Sn(Fe)	12c	0	0	0.1463(1)	0.29(2)	1
P	18e	0.2907(6)	0	0.25	0.7(2)	1
O(1)	36f	0.1920(5)	0.987(1)	0.1920(4)	0.19(2)	1
O(2)	36f	0.1869(8)	0.1617(8)	0.0825(4)	0.19(2)	1

TABLE IV. Powder diffraction data of $CdSnFe(PO_4)_3$ ($Cu\,K\alpha_1$; $\lambda = 1.540\,56$ Å).[a]

hkl	d_{obs} (Å)	$100I/I_0$ (obs)	$100I/I_0$ (calc)	*hkl*	d_{obs} (Å)	$100I/I_0$ (obs)	$100I/I_0$ (calc)
012	6.1299	5	5	318	1.6405	10	10
104	4.3766	4	3	140	1.6228	9	9
110	4.2936	100	100	413	1.5833	1	1
113	3.6901	40	40	048	1.5325	4	4
006	3.6088	3	3	0 1 14	1.5142	6	6
202	3.5168	12	12	1 3 10	1.4539	2	2
024	3.0500	6	6	416	1.4801	9	9
211	2.7875	7	6	0 3 12	1.4589	2	2
116	2.7626	75	75	238	1.4433	4	4
211	2.7206	6	5	330	1.4312	5	5
018	2.5434	6	6	2 0 14	1.4280	6	6
300	2.4789	18	17	4 0 10	1.4106	1	1
208	2.1883	8	8	1 1 15	1.3683	1	1
220	2.1468	6	6	1 2 14	1.3551	7	7
119	2.0988	2	2	511	1.3332	1	1
036	2.0433	7	7	336	1.3304	3	3
128	1.9497	20	21	514	1.2968	1	1
226	1.8450	25	25	428	1.2473	2	2
0 0 12	1.8044	3	3	600	1.2395	3	3
404	1.7584	2	1	3 1 14	1.2374	4	4
137	1.7161	1	2	250	1.1908	2	2
2 1 10	1.7112	3	3	2 3 14	1.1459	5	5
232	1.6853	1	1	526	1.1309	2	2
1 1 12	1.6635	1	1	348	1.1142	4	4

[a]Diffraction lines with $I_{obs} < 1$ are omitted.

Sn, Fe, and P sites in $[Cd]_{M1}SnFe(PO_4)_3$ (2.0 for Cd in M1 site, 3.8 for Sn/Fe, and 5.0 for P) are relatively consistent with the expected formal oxidation state of Cd^{2+}, Fe^{3+}, Sn^{4+} and P^{5+} ions. X-ray powder diffraction data of $CdSnFe(PO_4)_3$, obtained from the "observed intensities" of the Rietveld refinement ($Cu\,K\alpha 1$: 1.54056 Å), are given in Table IV.

D. Structure of $CaSnFe(PO_4)_3$

A preliminarily comparison between the powder XRD spectrum, for $CaSnFe(PO_4)_3$, presented in this work (Figure 4) with that already signalized in literature (PDF number 31-275) shows: (i) a notable difference in diffraction lines intensity and also (ii) the presence of additional weak diffraction lines in the present XRD spectrum (see, e.g., at $2\theta = 14.378°$ and $2\theta = 25.307°$) (Figure 4). Since the hexagonal cell parameters already mentioned ($a = 8.596$ Å, $c = 22.104$ Å) are relatively comparable to that calculated in the present work [$a = 8.569(1)$ Å, $c = 22.037(2)$ Å], and the observed additional diffraction lines have only a weak intensity, substantial improvement on the known literature data is probably related to the condition of the spectrum run (e.g., the counting time,...) and/or the way used for estimating the relative peak intensity. Taking into account the above-mentioned consideration, and in order to have more structural information about compounds with general formula $ASnFe(PO_4)_3$ (A = Ca,Sr,Ba), the structure determination of the selected $CaSnFe(PO_4)_3$ phosphate was undertaken.

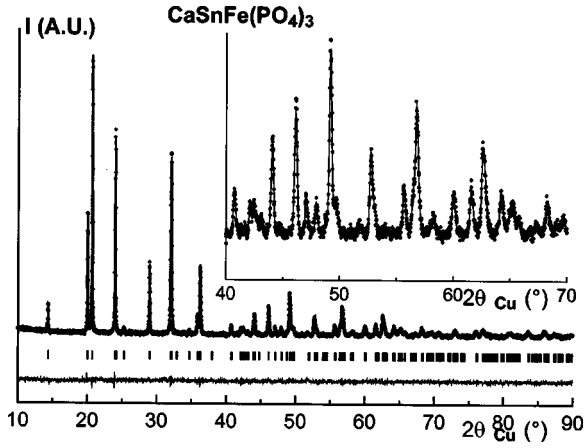

Figure 4. Experimental (···) calculated (—), and difference profile of the XRD pattern of $CaSnFe(PO_4)_3$.

Structural refinement of $CaSnFe(PO_4)_3$ was made in two principle steps. In the first step all calcium ions were supposed to occupy the M1 sites and Sn(Fe) within the Nasicon framework. This refinement was appropriate as shown by the good agreement between experimental and calculated intensity data (Figure 4). In the second step of refinement, and in order to confirm the last cationic distribution, two main hypotheses of refinement were verified: (i) all tin atoms in M1 sites ($[\square_3]_{M2}[Sn]_{M1}CaFe(PO_4)_3$) crystallographic formula) and (ii) all iron atoms in M1 sites ($[\square_3]_{M2}[Fe]_{M1}SnCa(PO_4)_3$ crystallographic formula). In both cases, large values of the displacement parameters for Sn and Fe in M1 sites ($B_{iso}(Sn)_{M1} = 29.3$ Å^2; $B_{iso}(Fe)_{M1} = 7.3$ Å^2), and negative values for cations within the framework ($B_{iso}(Ca/Fe) = -2.3(1)$ Å^2; $B_{iso}(Sn/Ca) = -0.3(1)$ Å^2) were obtained. Note for example that the Bragg reliability factors values are 19% and 7%, respectively, for $[\square_3]_{M2}[Sn]_{M1}CaFe(PO_4)_3$ and $[\square_3]_{M2}[Fe]_{M1}SnCa(PO_4)_3$ crystallographic formula. As

TABLE V. Results of the Rietveld refinement of $CaSnFe(PO_4)_3$.

$CaSnFe(PO_4)_3$
Space group, $R\bar{3}c$; [$Z=6$; $a_{hex}=8.569(1)$ Å; $c_{hex}=22.037(2)$ Å; $V=1401(1)$ Å^3]
Experimental data
Temperature, 298 K; angular range, $10° \leqslant 2\theta \leqslant 90°$; step scan increment ($2\theta$): 0.02°
Zero point (2θ), $-0.044(2)°$; number of fitted parameters, 28
Profile parameters
Pseudo-Voigt function, $PV=\eta L+(1-\eta)G$; $\eta=0.493(4)$
Polynomial function for the background (six parameters)
Half-width parameters, $U=0.207(5)$, $V=-0.013(6)$, and $W=0.005(1)$
Conventional Rietveld *R*-factors, $R_{WP}=4.3\%$; $R_P=3.3\%$; $R_B=3.3\%$; $R_F=3.7\%$

Atom	Site	Wyckoff positions			B_{iso} (Å^2)	Occupancy
Ca	6b	0	0	0	1.4(1)	1
Sn(Fe)	12c	0	0	0.1473(1)	0.40(3)	1
P	18e	0.2919(5)	0	0.25	0.7(1)	1
O(1)	36f	0.1869(7)	0.9800(8)	0.1928(3)	0.4(1)	1
O(2)	36f	0.1857(6)	0.1651(8)	0.0842(3)	0.4(1)	1

was expected, unacceptable BVS values were obtained from the two hypotheses of cationic distributions ($[\square_3]_{M2}[Sn]_{M1}CaFe(PO_4)_3$, e.g., BVS=2.75 for Sn^{4+} ions) and ($[\square_3]_{M2}[Fe]_{M1}SnCa(PO_4)_3$; e.g. BVS=0.86 for Fe^{3+} ions). It should be noticed that refinement with simultaneous occupation of both M1 and M2 site by Ca^{2+} ions leads to a small and physically insignificant value of the occupancy factor in M2(18e) sites. The final reliability factors and atomic parameters for $[\square_3]_{M2}[Ca]_{M1}SnFe(PO_4)_3$ are given in Table V. Ca–O(2) [2.393(2) Å] and Sn(Fe)–O [1.968(2); 2.054(2) Å] interatomic distances agree well with the ionic radii values in six coordination ($r_{Ca^{2+}}=1.00$ Å).

TABLE VI. Powder diffraction data of $CaSnFe(PO_4)_3$ (Cu $K\alpha_1$; $\lambda=1.540\,56$ Å).[a]

hkl	d_{obs} (Å)	$100I/I_0$ (obs)	$100I/I_0$ (calc)	*hkl*	d_{obs} (Å)	$100I/I_0$ (obs)	$100I/I_0$ (calc)
012	6.1558	8	8	1 3 10	1.5042	9	9
104	4.4235	45	45	146	1.4817	9	9
110	4.2844	100	100	0 3 12	1.4745	2	2
113	3.7009	75	75	2 0 14	1.4491	7	7
202	3.5164	1	1	238	1.4482	2	2
024	3.0775	26	26	3 1 11	1.4356	1	1
116	2.7885	66	66	054	1.4331	3	3
211	2.7824	9	9	330	1.4281	5	5
018	2.5824	3	3	4 0 10	1.4192	4	3
214	2.4995	10	10	1 1 15	1.3897	3	3
300	2.4736	19	19	1 2 14	1.3727	8	8
208	2.2117	5	6	244	1.3591	2	2
220	2.1422	4	4	3 2 10	1.3472	3	3
119	2.1259	4	4	336	1.3311	3	3
1 0 10	2.1125	2	2	511	1.3304	1	1
217	2.0942	1	1	514	1.2955	6	6
223	2.0565	2	2	0 2 16	1.2912	1	1
036	2.0517	8	8	3 1 14	1.2503	5	5
128	1.9653	19	19	428	1.2498	1	1
134	1.9280	6	6	600	1.2368	4	4
0 2 10	1.8947	6	5	2 1 16	1.2333	1	1
226	1.8505	31	31	517	1.2274	1	1
0 0 12	1.8364	4	4	0 0 18	1.2243	2	2
042	1.8295	3	3	250	1.1883	2	2
2 1 10	1.7328	16	15	2 4 10	1.1831	2	2
137	1.7227	3	4	2 3 14	1.1558	6	6
318	1.6488	9	9	5 1 10	1.1907	3	3
324	1.6266	7	7	526	1.1306	4	4
140	1.6194	12	12	348	1.1155	4	4
235	1.5881	1	1	1 5 11	1.1097	1	1
413	1.5814	2	2	164	1.1086	1	1
0 1 14	1.5398	6	5	0 1 20	1.0899	3	2
048	1.5350	3	3				

[a]Diffraction lines with $I_{obs}<1$ are omitted.

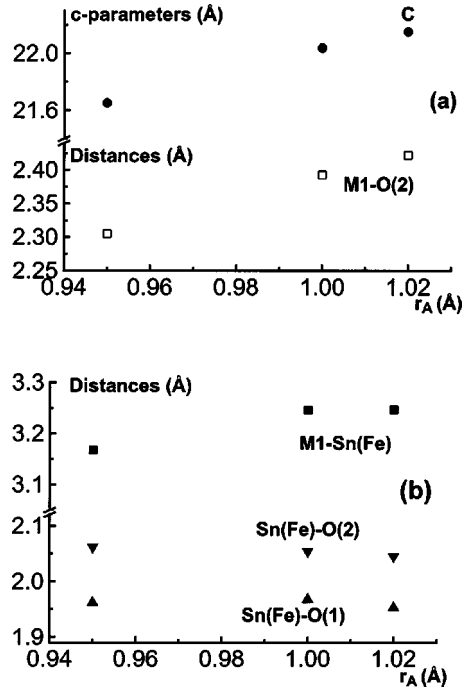

Figure 5. Evolution, with A ionic radii (r_A), of *c* parameters and interatomic distances in $ASnFe(PO_4)_3$ ($A=Na_2$,Ca,Cd) materials.

P–O distance values, 1.508(2) and 1.538(2) Å, match well with those typically observed in Nasicon-type phosphates. The calculated BVS values for Ca, Sn, Fe, and P sites in $[\square]_{M2}[Ca]_{M1}SnFe(PO_4)_3$ (1.9 for Ca, 3.8 for Sn/Fe, and 5.1 for P) are consistent with the expected formal oxidation state of Ca^{2+}, Fe^{3+}, Sn^{4+}, and P^{5+} ions. X-ray powder diffraction data of $CaSnFe(PO_4)_3$, obtained from the ''observed intensities'' of the Rietveld refinement ($Cu\,K\alpha 1$: 1.540 56 Å), are presented in Table VI.

IV. GENERAL DISCUSSION

Close examination of the atomic positions and interatomic distances shows that the main differences between both $CdSnFe(PO_4)_3$ and ($Na_2SnFe(PO_4)_3$ or $CaSnFe(PO_4)_3$) structures are in the ribbons parallel to the *c* axis. The linear increases of M1–O(2) distance versus A cation ionic radii (r_A), in $ASnFe(PO_4)_3$ ($A=Na_2$,Ca,Cd) phases, is accompanied with a regular increase of c_{hex} parameters [Figure 5(a)]. The increase of the M1 site size in $Na_2SnFe(PO_4)_3$ is accompanied by oxygen displacements perpendicular to the *c* axis which give rise to rotation of the PO_4 tetrahedra and leads to a distortion of the $[Sn(Fe)\times(PO_4)_3]$ framework. On the other hand, as a result of the electrostatic repulsion between A cations ($A=Cd,Ca,Na_2$) in M1 site and neighbouring $Sn^{4+}(Fe^{3+})$ cations in $ASnFe(PO_4)_3$ phases, the Sn(Fe)–O(2) distance in $Sn(Fe)O_6$ octahedra is larger than Sn(Fe)–O(1) one and consequently, the O(1)–Sn(Fe)–O(1) (α_1) angle is higher than the O(2)–Sn(Fe)-O(2) (α_2) one [Figures 1(a) and 5(b)] (i.e., $\alpha_1=97.5°$ and $\alpha_2=78.0°$ for $CdSnFe(PO_4)_3$; $\alpha_1=96.3°$ and $\alpha_2=79.2°$ for $CaSnFe(PO_4)_3$; and $\alpha_1=93.7°$ and $\alpha_2=80.3°$ for $Na_2SnFe(PO_4)_3$). As can be deduced from the relatively small variation of Sn(Fe)–O distances versus r_A in $ASnFe(PO_4)_3$ ($A=Cd,Ca,Na_2$) phases [Figure 5(b)], the volume occupied by $Sn(Fe)O_6$ octahedra is comparable and agrees well with hypothesis of Sn(Fe) distribution only within the $[Sn(Fe)PO_4)_3]$ Nasicon framework.

V. CONCLUSION

The localisation, of Na^+ within M1 and M2 sites of $Na_2SnFe(PO_4)_3$, and Ca^{2+} in M1 sites of $CaSnFe(PO_4)_3$, has been proved from powder X-ray diffraction data. In the case of $CdSnFe(PO_4)_3$, XRD data cannot distinguish, without difficulty, between the two isoelectronic Cd^{2+} and Sn^{4+} cations but analysis of cation–anion distances found after structure determination permits a conclusion about the cationic distribution. In the case of $ASnFe(PO_4)_3$ ($A=Cd,Ca$) materials, the present example of structural analysis shows how the overall set of distance values, found after structural refinements, and calculated bond valence sums (BVS) can give effective support for structural determination when it is difficult to distinguish, from powder XRD data, between elements of neighbouring atomic number in the periodic table.

Aatiq, A., Delmas, C., El Jazouli, A., and Gravereau, P. (**1998**). ''Structure and electrochemical study of $Li_{2x}Mn_{(1-x)}TiCr(PO_4)_3$ ($x=0-0.5$) with Nasicon-like structure,'' Ann. Chim. Sci. Mat., **23**, 121–124.

Aatiq, A. and Dhoum, H. (**2003**). ''Structure of $AFeTi(PO_4)_3$ ($A=Ca,Cd$) Nasicon phases from powder X-ray data,'' Powder Diffr., (in press).

Aatiq, A., Ménétrier, M., Croguennec, L., Suard, E., and Delmas, C. (**2002a**). ''On the structure of $Li_3Ti_2(PO_4)_3$,'' J. Mater. Chem. **12**, 2971–2978.

Aatiq, A., Ménétrier, M., El Jazouli, A., and Delmas, C. (**2002b**). ''Structural and lithium intercalation studies of $Mn_{(0.5-x)}Ca_xTi_2(PO_4)_3$ phases ($0\leqslant x\leqslant 0.50$),'' Solid State Ionics **150**, 391–405.

Brown, I. D. and Altermatt, D. (**1985**). ''Bond-valence parameters obtained from a systematic analysis of the inorganic crystal structure database,'' Acta Crystallogr., Sect. B: Struct. Sci. **41**, 244–247.

Delmas, C., Nadiri, A., and Soubeyroux, J. L. (**1988**). ''The Nasicon-type titanium phosphates $ATi_2(PO_4)_3$ ($A=Li,Na$) as electrode materials,'' Solid State Ionics **28–30**, 419–423.

Delmas, C., Viala, J. C., Olazcuaga, R., Le Flem, G., Hagenmuller, P., Cherkaoui, F., and Brochu, R. (**1981**). ''Ionic conductivity in Nasicon-type phases $Na_{1+x}Zr_{2-x}L_x(PO_4)_3$ ($L=Cr,In,Yb$),'' Solid State Ionics **3/4**, 209–214.

Hagman, L. and Kierkegaard, P. (**1968**). ''The crystal structure of $NaMe^{IV}_2(PO_4)_3$; Me=Ge, Ti, Zr,'' Acta Chem. Scand. **22**, 1822–1932.

Hong, H. Y-P. (**1976**). ''Crystal structures and crystal chemistry in the system $Na_{(1+x)}Zr_2Si_xP_{(3-x)}O_{12}$,'' Mater. Res. Bull. **11**, 173–182.

Isasi, J. and Daidouh, A. (**2000**). ''Synthesis, structure and conductivity study of monovalent phosphates with the langbeinite structure,'' Solid State Ionics **133**, 303–313.

Kasthuri Rangan, K. and Gopalakrishnan, J. (**1994**). ''New titanium-vanadium phosphates of Nasicon and Langbeinite structures, and differences between the two structures toward deintercalation of alkali metal,'' J. Solid State Chem. **109**, 116–121.

Krimi, S., Mansouri, I., El Jazouli, A., Chaminade, J. P., Gravereau, P., and Le Flem, G. (**1993**). ''The structure of $Na_5Ti(PO_4)_3$,'' J. Solid State Chem. **105**, 561–566.

Masquelier, C., Wurn, C., Rodriguez-Carvajal, J., Gaubicher, J., and Nazar, L. F. (**2000**). ''A powder neutron diffraction investigation of the two rhombohedral Nasicon analogues: γ-$Na_3Fe_2(PO_4)_3$ and $Li_3Fe_2(PO_4)_3$,'' Chem. Mater. **12**, 525–532.

Morin, E., Angenault, J., Couturier, J. C., Quarton, M., He, H., and Klinowski, J. (**1997**). ''Phase transition and crystal structures of $LiSn_2(PO_4)_3$,'' Eur. J. Inorg. Chem. **34**, 947–958.

Padhi, A. K., Nanjundaswamy, K. S., Masquelier, C., and Goodenough, J.B. (**1997**). ''Mapping of transition metal redox energies in phosphates with NASICON structure by lithium intercalation,'' J. Electrochem. Soc. **144**, 2581–2586.

Rodriguez-Carvajal, J. (**1997**). ''Fullprof, Program for Rietveld refinement,'' Laboratoire Léon Brillouin (CEA-CNRS) Saclay, France.

Shannon, R. D. (**1976**). ''Revised effective ionic and systematic studies of interatomic distances in halides and chalcogenides,'' Acta Crystallogr., Sect. A: Cryst. Phys., Diffr., Theor. Gen. Crystallogr. **A32**, 751–767.

Woodcock, D. A., Lightfoot, P., and Smith, R. I. (**1999**). ''Powder neutron studies of three low thermal expansion in the NZP family: $K_{0.5}Nb_{0.5}Ti_{1.5}(PO_4)_3$, $BaTi_2(PO_4)_3$ and $Ca_{0.25}Sr_{0.25}Zr_2(PO_4)_3$,'' J. Mater. Chem. **9**, 2631–2636.

Yin, S. C., Grondey, H., Strobel, P., Anne, M., and Nazar, L. F. (**2003**). ''Electrochemical property: Structure relationships in monoclinic $Li_{3-y}V_2(PO_4)_3$,'' J. Am. Chem. Soc. **125**, 10402–10411.